Capabilities of UV Coronagraphic Spectroscopy for Studying the Source Regions of SEPs & the Solar Wind

Leonard Strachan, John Raymond, John Kohl, Steven Cranmer, Larry Gardner, & Jun Lin
Harvard-Smithsonian Center for Astrophysics, Cambridge, MA 02138

Solar & Space Physics and the Vision for Space Exploration
Wintergreen, VA, October 16-20, 2005

Coronal Mass Ejections (CMEs), Flares, & Solar Energetic Particles (SEPs):

What is the role of current sheets in the production of solar flares and CMEs?
What are the physical processes controlling the impulsive and gradual production of SEPs?

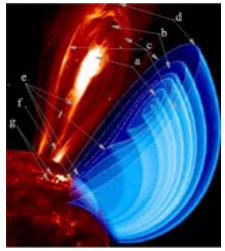

Theory and Model of Solar Flares, Eruptive Prominences, and CMEs

- The closed magnetic field in low corona is highly stretched by the eruption and a current sheet forms separating magnetic fields of opposite polarities.
- The temporal vacuum due to the eruption near the current sheet drives plasma and magnetic field towards the current sheet invoking the driven magnetic reconnection inside the current sheet.
- Magnetic reconnection produces flare ribbons on the solar surface and flare loops in the corona, and helps CME to escape smoothly.
- The charged particles can be accelerated either by the electric field in the current sheet induced by the magnetic reconnection inflow, or by the shock driven by CME.

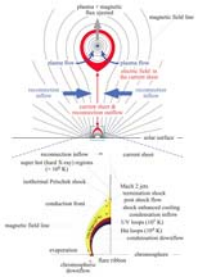

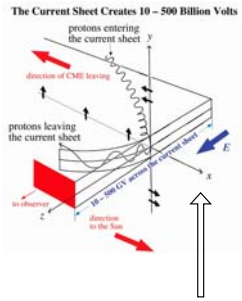

UVCS Observational Evidence of the Predicted Hot Current Sheet

- Several CME current sheets have been observed with UVCS, EIT, and LASCO (e.g., Ko et al. 2003).
- UVCS found **6 million K** gas, which is consistent with models predicting that magnetic energy is converted into heating & acceleration of the CME.
- Coordinated Ulysses & SOHO observations of another CME in Nov. 2002 found similar high Fe charge states both in the corona and at 4 AU—thus following for the first time hot parcels of CME plasma from their origin to interplanetary space (Poletto et al. 2004).

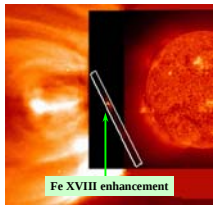

Reconnection Inflow near the CME/Flare Current Sheet Observed in Lyα

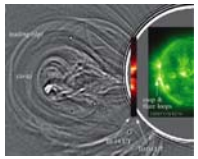

- On Nov. 18, 2003, a CME exhibited a central depression in H I Lyman alpha that "closed down" as a function of time, indicating the **inflow reconnection speed.** (Slit image above contains 5 exposures: time goes from right to left)

Electric Field in Current Sheet & SEPs

UVCS demonstrated potential for spectroscopic measurements of **E**-fields:

$|\mathbf{B}|$: determined from energy balance, using measured thermal & kinetic energy densities in current sheet.

V_{in}: determined from Lyα inflow motions (see left) or white-light blob V_{out} (with mass conservation).

$$|\mathbf{E}| = \frac{|\mathbf{v}_{in} \times \mathbf{B}|}{c}$$

- Voltage drop across the current sheet as a result of ***E*** reaches 10–500 GV.
- A residual magnetic field inside the current sheet $\delta\boldsymbol{B}$ is along the positive *y* direction. It is small compared to ***B***, but it is crucial for turning particles accelerated in *z* direction about the *y* direction and ejecting the particles from the current sheet.
- The energy gain of accelerated particles is proportional to $|\delta\boldsymbol{B}|^{-2}$. With the vanishing of $\delta\boldsymbol{B}$, the energy gain goes to infinity and the particles never come out of the current sheet (see, e.g., Speiser 1965; Priest & Forbes 2000). The energy gain is independent of q/m to 2nd approximation.

CME-Driven Shock Waves and SEPs

- UV spectroscopic diagnostics can determine the parameters describing the shock itself and the pre- and post-shock plasma.
- These parameters are needed as inputs to SEP acceleration models for specific events.

Required parameters:

Pre-shock	Post-shock
n(r,θ) T_e , T_{ion} $f_e(v)$, $f_p(v)$ q, composition V_A , θ	V_{shock} , $\vec{V}_{plasma}$ T_e , T_{ion} compression ratio / Mach number

Shock onset: height, |B|

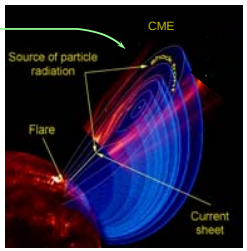

CME Shock Diagnostics

- **Pre-CME density, temperatures, composition**: UVCS has measured these prior to 4 observed shocks.
- **Post-shock ion temperatures:** UVCS has measured high temperatures of shock-heated plasma ($T_p \approx T_{ion}$)
- **Shock onset radius:** The high temperatures (at specific radii) from UVCS indicate the shock has formed; Type II radio bursts give the density at which the shock forms.
- **Shock speed:** UVCS density measurements allow the Type II density vs. time to be converted to shock speed ($V_{shock} > V_{CME}$)
- **Shock compression ratio & Mach number:** UVCS can measure the density ratio and the adiabatic proton temperature ratio (Lya), from which the Mach number can be derived.
- **Magnetic field strength at onset radius:** At the onset radius, Mach number = 1, so measuring V_{shock} gives V_{Alfven}, and thus B in the pre-shock corona (e.g., Mancuso et al. 2003).

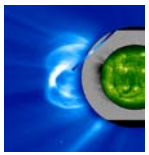

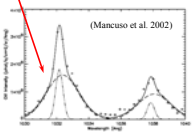

Future Diagnostics and Instrument Concepts:

Measuring Electron Velocity Distribution from Thomson-scattered Lyman alpha

- This technique has been tested successfully by UVCS in a bright streamer (Fineschi et al. 1998). Below we plot simulated H I Lyα broadening from both H^0 motions (yellow) and electron Thomson scattering (green). With sufficient sensitivity, **both proton and electron temperatures can be measured.**

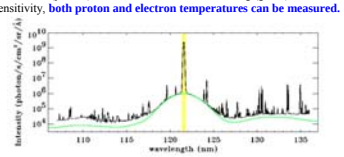

Electron Velocity Distribution Path

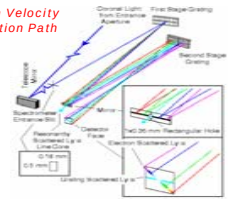

Coronal Magnetic Field Measurements in Post-Flare Loops

The Hanle effect produces a rotation of polarization angle (β) for scattering in magnetic field **B**:

$\beta = \frac{1}{2} \tan^{-1} (2\, \omega_L / A_{12})$, where $\omega_L = eB/(2\, m_e)$ i.e. the Larmor frequency, and A_{12} is the Einstein A-value for the line.

Expected Exposure Times:

For **R = 1.3 $R_\odot$** , |**B**| = 5 G, and plane of loop || LOS

t_{exp} = 3.8 min for H I Lyα
t_{exp} = 6.6 hrs for H I Lyβ
(time for 3 polarizer positions.)

Measured rotation angle:
17.2° ± 5.1° for H I Ly β
4.6° ± 1.4° for H I Ly α

Derived |**B**| = 5.0 ± 1.5 Gauss

Methodology:

|**B**| determined from polarization angle of H I Lyβ relative to H I Lyα (1° accuracy).

B direction from (P, β) determined from measurements of 2 spectral lines

EUV Polarimeters

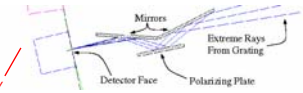

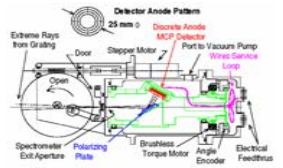

Improvements over UVCS on SOHO

A remote external occulter provides:

- Improved sensitivity (> 400 times UVCS at 1.5 R_o for Lyα and OVI).
- Improved spatial resolution (3.5 arcsec).

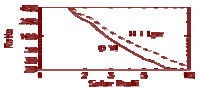

- Co-registered field of view extends down to 1.15 R_o for both UV and visible light
- Broader wavelength coverage for UV:

HeII Path: 48–74 nm first order 26–37 nm second order	EUV Path: 70–150 nm first order 38–75 nm second order

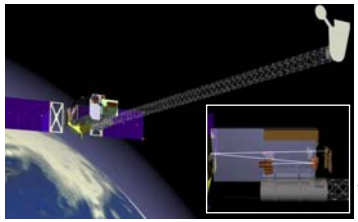

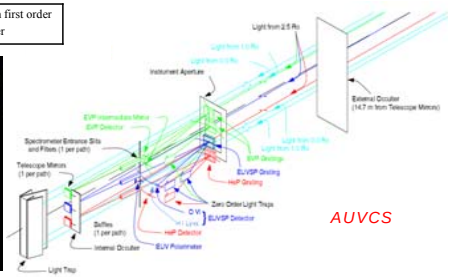

The Solar Wind:

What are the physical processes that control the heating and acceleration of fast and slow solar wind streams?

Initial UVCS results

- In June 1996, the first measurements of heavy ion (e.g., O^{+5}) line emission in the extended corona revealed **surprisingly wide** line profiles . . .

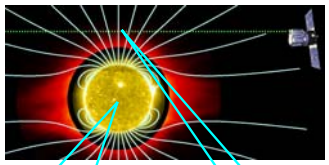

On-disk profiles: T = 1–3 million K
Off-limb profiles: **T > 200 million K !**
(see, e.g., Kohl et al. 1997, 1998; Noci et al. 1997; Cranmer et al. 1999)

The Impact of UVCS/SOHO

UVCS/SOHO has led to new views of the acceleration regions of the solar wind. Key results (1996 to 2004) include:

- The fast solar wind becomes **supersonic** much closer to the Sun (2-3 R_o) than previously believed (Kohl et al. 1998).
- In coronal holes, heavy ions (e.g., O^{+5}) both flow **faster** and are **heated** hundreds of times more strongly than protons and electrons, and have **anisotropic temperatures**.
- Ulysses/SOHO quadrature observations demonstrate the ability to trace absolute abundances and other plasma parameters back to the corona (Poletto et al. 2002, 2004).
- The slow wind from **streamers** flows mostly along the open-field "edges," exhibiting similar high temperatures and anisotropies as coronal holes—suggesting similar physics as the fast wind (Strachan et al. 2002; Frazin et al. 2003).

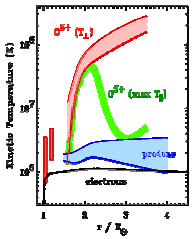

Identifying Fundamental Physical Processes

- UVCS observations have **rekindled theoretical efforts** to understand heating and acceleration of the plasma in the acceleration region of the solar wind (see Cranmer 2000, 2002; Hollweg & Isenberg 2002).
- Measured ion properties strongly suggest a specific type of (collisionless) waves in the corona to be damped: ion cyclotron waves with frequencies of 10 to 10,000 Hz.
- It is still not clear how these waves can be generated from the much lower-frequency Alfven waves known to be emitted by the Sun (5 min. periods), but **MHD turbulence** and **kinetic instability** models are being pursued by several groups.
- Low frequency Alfven waves may provide some fraction of the primary heating, which can be constrained observationally as well (e.g., Cranmer & van Ballegooijen 2005).

Ion cyclotron resonance:

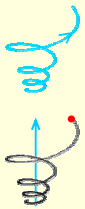

The Need for Better Observations

Even though UVCS/SOHO has made significant advances,

- We still do not understand the **physical processes** that heat and accelerate the entire plasma (protons, electrons, heavy ions),

(Our understanding of ion cyclotron resonance is based essentially on just one ion!)

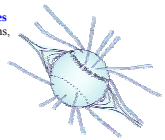

- There is still controversy about whether the fast solar wind occurs primarily in dense **polar plumes** or in low-density inter-plume plasma,

- We still do not know how and where the various components of the variable **slow solar wind** are produced (e.g., "blobs;" Wang et al. 2000).

UVCS has shown that answering these questions is possible, but cannot make the required observations.

Solar Wind: Future Diagnostics

- Observing emission lines of **additional ions** (i.e., more *charge & mass* combinations) in the acceleration region of the solar wind would constrain the specific kinds of waves and the specific collisionless damping modes.
- Measuring **electron temperatures** above ~1.5 R_s (never done directly before) would finally allow us to determine the heating and acceleration rates of solar wind electrons vs. distance.
- Measuring **non-Maxwellian velocity distributions** of electrons and positive ions would allow us to test specific models of, e.g., velocity filtration, cyclotron resonance, and MHD turbulence.

Greater photon sensitivity and an expanded wavelength range would allow all of the above measurements to be made, thus allowing us to determine the **relative contributions of different physical processes** to the heating and acceleration of all solar wind plasma components.